Arch. Metall. Mater. **65** (2020), 2, 595-600

DOI: 10.24425/amm.2020.132797

MOHAMMAD SABET[1*], KAMRAN MAHDAVI[1], FAHIMEH SALMEH[2]

HYDROTHERMAL SYNTHESIS OF HIGHLY UNIFORM CHALCOPYRITE $CuFeS_2$ NANOPARTICLES

In this research work, high uniform $CuFeS_2$ chalcopyrite with 20-40 nm particles were synthesized via a simple hydrothermal method. Different analysis were used to characterize the obtained product such as X-ray diffraction pattern (XRD), scanning electron microscopy (SEM), transmission electron microscopy (TEM) and thermal gravimetric analysis (TGA). The photocatalytic activity of the product was investigated by degradation three different dyes namely acid brown, acid red and methylene blue. The results showed the synthesized $CuFeS_2$ nanoparticles have high photocatalytic activity and can degrade the used dyes in large quantities.

Keywords: Chalcopyrite; Uniform; Nanoparticles; Hydrothermal; $CuFeS_2$

1. Introduction

One of the I-III-VI_2 ternary compound that is a semiconductor is known as chalcopyrite copper iron sulfide ($CuFeS_2$) [1]. It has unique properties such as high Neel temperature and advanced electrical and optical properties [2] with an unusually low optical band gap of 0.53 eV [3]. It can be used in batteries [4], thermoelectric devices [5] and solar cells [6]. Until now many efforts have been done for synthesis of $CuFeS_2$ with different morphologies such as nanosheets [7], nanoparticles [8], nanowires [9] and spherical [10] by using various methods such as hydrothermal [11], solvothermal [12] and thermal decomposition [13]. Hu and et al [14] used from hydrothermal method to synthesis of $CuFeS_2$ nanorod. Also colloidal $CuFeS_2$ chalcopyrite was synthesized by J. Silvester and et al [15]. It has a useful bandgap and unique properties such as thermoelectricity and ferroelectricity [16]. Hydrothermal method is a simple way to synthesis of high-quality nanostructures due to its high temperature medium that can lead to synthesis of highly crystalline and pure materials. In this research work, high uniform chalcopyrite $CuFeS_2$ nanoparticles were synthesized via a simple hydrothermal method. To obtain high uniform nanoparticles, a surfactant was used to prevent them from aggregation. The synthesized nanoparticles were used to degradation of Acid Red and Acid Brown to evaluate the photocatalytic activity.

2. Experimental

All the precursors such as $CuCl_2$, ethylenediamine, thiourea, $FeSO_4$ and polyvinylpyrrolidone (PVP) were purchased from Merck compony in the high purity grade and used as received. To characterize the product different analysis were served. XRD patterns were recorded by a Rigaku D-max C III, X-ray diffractometer using Ni-filtered Cu Kα radiation. Scanning electron microscopy (SEM) images were obtained on Zeiss (Sigma VP) equipped with an energy dispersive X-ray spectroscopy. UV-Vis spectra were recorded using a UV-Vis spectrophotometer (PerkinElmer, Lambda 650). Transmission electron microscopy (TEM) images were obtained on zeiss transmission electron microscope (Zeiss-EM10C-100 KV). Fourier transform infrared (FT-IR) spectra were recorded on Shimadzu Varian 4300 spectrophotometer in KBr pellets. Thermal gravimetric analysis (TGA) was analyzed by Netzsch STA449F3A-1517-M under argon atmosphere (25°C/10.0(K/min)/1200°C). The experimental procedure was done by dissolving 0.7654 g of $CuCl_2$, 0.6785 g (0.89 M) of $SC(NH_2)_2$ and 1.058 g (of $FeSO_2$ in 20, 10 and 10 ml of deionized water. After that three obtained solutions were added together and stirred for 30 min. Then PVP was poured to the solution with 1:1 mole ratio respect to $CuCl_2$ reagent, and stirred for 10 min. After that the solution was mixed with 80 ml of glacial ethylenediamine. The final solution was moved to the autoclave and inserted in the oven and heated at 190°C for 32 h.

[1] VALI-E-ASR UNIVERSITY OF RAFSANJAN, FACULTY OF SCIENCE, DEPARTMENT OF CHEMISTRY, RAFSANJAN, PO BOX: 77176, IRAN
[2] VALI-E-ASR UNIVERSITY OF RAFSANJAN, FACULTY OF SCIENCE, DEPARTMENT OF PHYSICS, RAFSANJAN, PO BOX: 77176, IRAN

* Corresponding author: M.sabet@vru.ac.ir

the obtained powder was washed with HCl, ethanol and distilled water to remove any unreacted materials. Finally, the powder was dried at 60°C for 24 h and was investigated by different analysis.

3. Results and discussion

3.1. XRD pattern

XRD analysis of the product is shown in Fig. 1. It can be seen that the XRD analysis showed three peaks at 29.7°, 49.2° and 58.1°, that reflect (112), (220) and (312) miller indices and completely matches with JCPDS No. 00-001-0842. Also, it was found the product has tetragonal phase with $a = b = 5.24$ A° and $c = 10.30$ A° lattice parameters. The crystallite size was calculated by Scherrer's formula ($D_{hkl} = (K \cdot \lambda)/(\beta \cdot \cos\theta)$). In the Scherrer's formula, D_{hkl} is the volume weighted crystallite size (nm); K is the shape factor ($K = 0.9$); λ is the wavelength of the X-rays ($\lambda = 0.154056$ nm for $CuK_{\alpha 1}$ radiation); θ is the Bragg diffraction angle; β is the broadening of the *h*kl diffraction peak measured at half of its maximum intensity (in radians) [17]. The calculated crystallite size was 45.5 nm that is agreed with TEM analysis. The XRD results showed the product is pure and there is no impurity in the product.

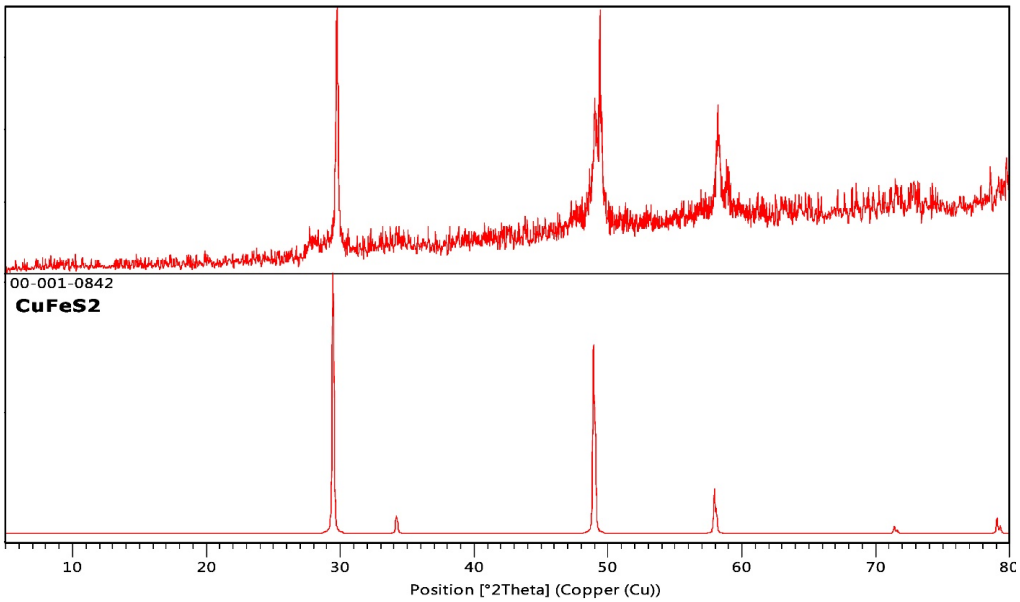

Fig. 1. XRD pattern of $CuFeS_2$ nanoparticles

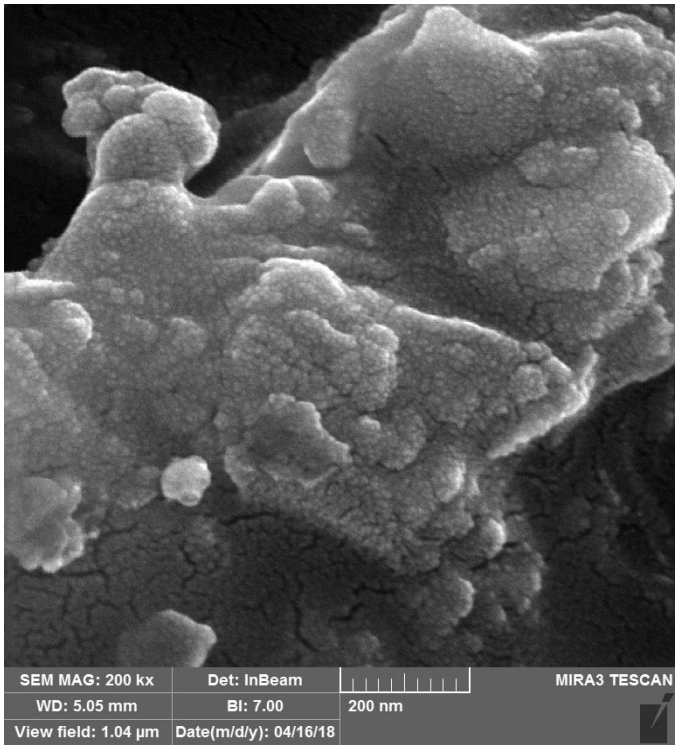

Fig. 2. SEM image of the synthesized chalcopyrite $CuFeS_2$

3.2. SEM and TEM images

Fig. 2 shows SEM images of the synthesized $CuFeS_2$ chalcopyrite. It can be observed that the synthesized $CuFeS_2$ nanoparticles is composed of 20-40 nm particles that are aggregated together. In fact due to huge active surface of the small particles, they aggregated together to decrease the surface energy. Due to aggregation of the particles, SEM can't show the particles size rightly; So, to study more about the product size and morphology, TEM analysis was used. TEM images and particle size histogram showed the product is composed of 20-40 nm uniform particles. As shown in Fig. 3, the particles are arranged in high order and the product has high uniformity. The main reason for synthesis of highly uniform $CuFeS_2$ nanoparticles in this research work is due to using PVP and ethylenediamine in the experimental procedure. In fact, these reagents act as surfactant materials besides their normal functional. When the $CuFeS_2$ nucleus are created, these molecules adhere to their surface and prevent them from further aggregations by creation a steric hindrance around

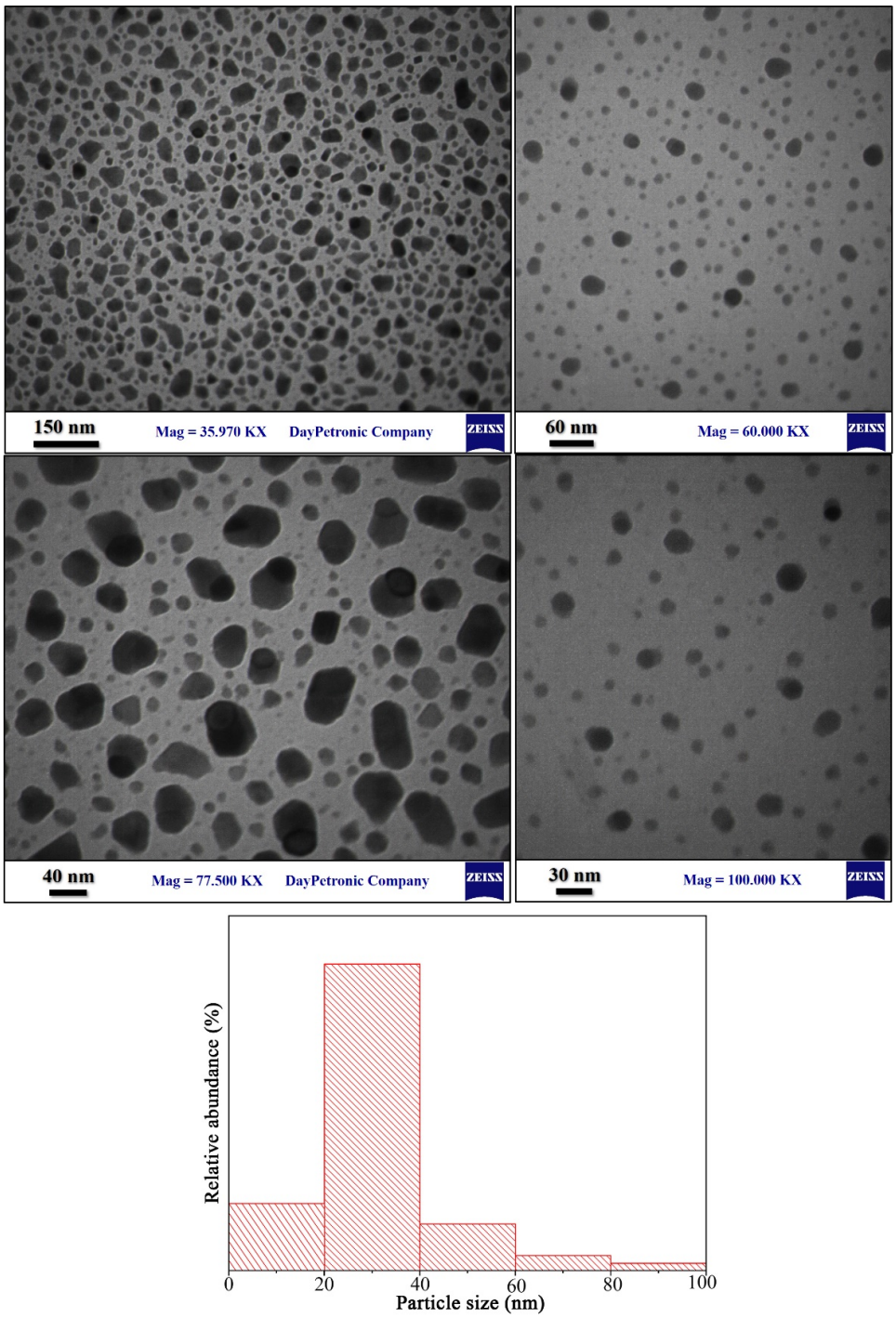

Fig. 3. TEM image and particle size histogram of the synthesized chalcopyrite $CuFeS_2$

the $CuFeS_2$ nucleus. Therefore, the synthesized $CuFeS_2$ can't be aggregated and hence highly uniform nanoparticles will be created. Scheme. 1 shows the surfactant performance to prevent the nucleus aggregation.

3.3. FT-IR analysis

To study the surface functional groups of the product, FT-IR analysis were served. It can be observed (Fig. 4) that the FT-IR shows different vibrational peaks. The peak placed at 1641 cm^{-1} can be attributed to N-H bending vibration. The peak placed at 1048 cm^{-1} is related to C-N stretching vibrations. Also N-H stretching vibration is appeared at 2931 cm^{-1}. The mentioned vibrational peaks confirm the presence of ethylenediamine on the CuFeS2 surface that approve this molecule act as capping agent in addition to solvent role and prevent the aggregation of the CuFeS2 particles. The peaks located at 1379 cm^{-1} and 3435 cm^{-1} are related to O-H bending and stretching vibrations, respectively that can be attributed to H_2O adsorption by the product surface. In fact, due to huge surface of the synthesized nanoparticles they can adsorb different molecules in the medium such as the air humidity.

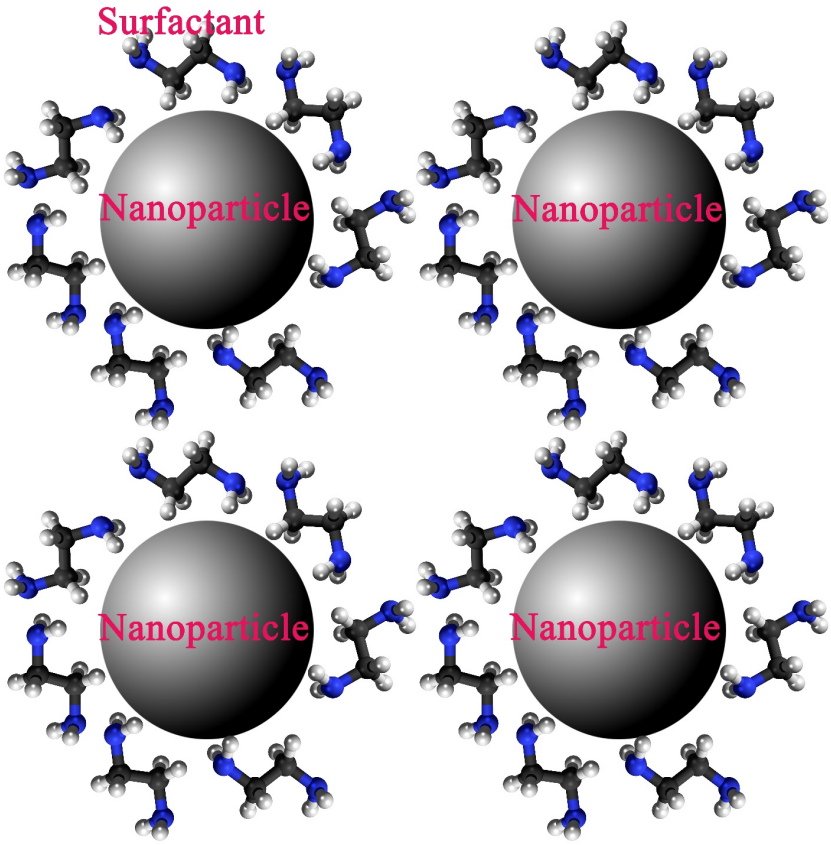

Scheme 1. The effect of surfactant on the product size and morphology

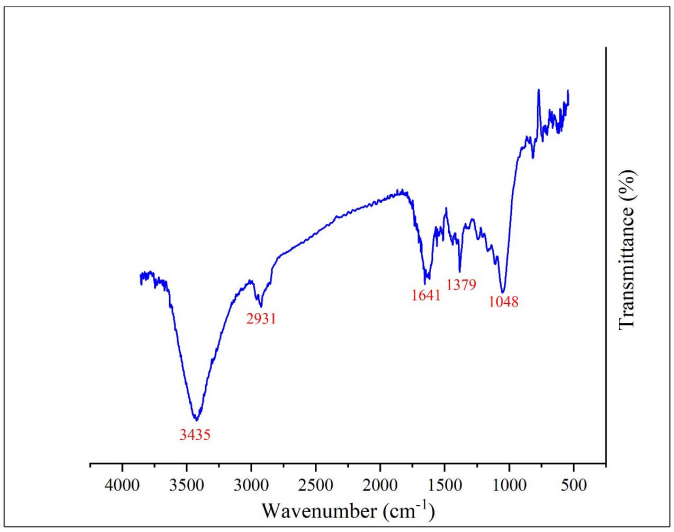

Fig. 4. FT-IR spectrum of the product

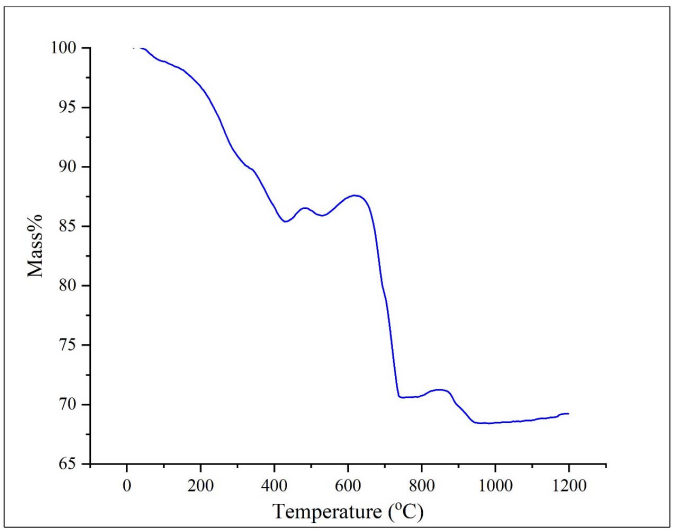

Fig. 5. TGA curve of the product

3.4. TGA analysis

Thermal stability of the product was studied by TGA analysis. As shown in Fig. 5, in two steps 30% of the product was lost. The first mass loss step can be related to losing water and surface groups such as surfactant. The other mass loss step that occur at 600°C can be attributed to decompose of $CuFeS_2$ to CuS and FeS. In fact, it can be said that the product can be stable until 600°C and after that it can decompose to CuS and FeS.

3.5. Photocatalytic activity

The photocatalytic activity of the product was studied by degradation of two dyes namely acid brown and acid red (Fig. 6). The results showed the product has high photocatalytic activity and it can degradation of the used dyes in the short time. In fact, due to high surface to volume ratio of the product, large amount of the dye molecules can adsorb on the nanoparticles surfaces and hence the large number of dye molecules can be decomposed

in the minimum time. Furthermore, when the synthesized nanostructures were exposed under UV irradaiation, the electron-hole pairs were created that can prepare reactive oxide species (ROS) such as OH radical in the aqueous solution that be used to decompose the selected dyes from a radical mechanism. In addition, by using PVP as surfactant, the nanoparticles surface defects were decreased and therefore the produced electron-hole pairs were increased that can enhance the product photocatalytic activity. Scheme 2 shows the mechanism of dye degradation in presence of $CuFeS_2$ photocatalyst.

Two compare our work with the other ones, a review of the works related to synthesis of $CuFeS_2$ has been mentioned. Lyubutin and et al [18] synthesized self-organized single-crystalline nanobricks of chalcopyrite $CuFeS_2$ and studied their magnetic properties. They used copper acetate monohydrate, iron acetate, sulfur powder, octadecylamine and trioctylphosphine under argon gas flow. Wang and et al [19] synthesized Single crystal of $CuFeS_2$ through solventothermal process. copper (II) ethyldithiocarbamate, iron ethyldithiocarbamate, the dithiocarbamate-based precursors, tri-octylphosphine, and oleylamine were used to synthesis of semiconducting $CuFeS_2$ nanocrystals by Wang and et al [13]. They found by selecting 100% excess sulfur, the product with more uniform morphology, stoichiometric composition and a narrow size distribution. Disale and et al [20] synthesized single-source precursors contain both copper and sulphur for synthesize of $CuFeS_2$ nanocrystals. Bhattacharyya and et al [8] synthesized $CuFeS_2$ Quantum Dots as well as core-shell structures with highly Luminescent and investigated their optical properties.

4. Conclusion

High uniform $CuFeS_2$ chalcopyrite nanoparticles were synthesized via a simple hydrothermal method. X-ray diffraction pattern (XRD) was used to determine the crystallinity of the

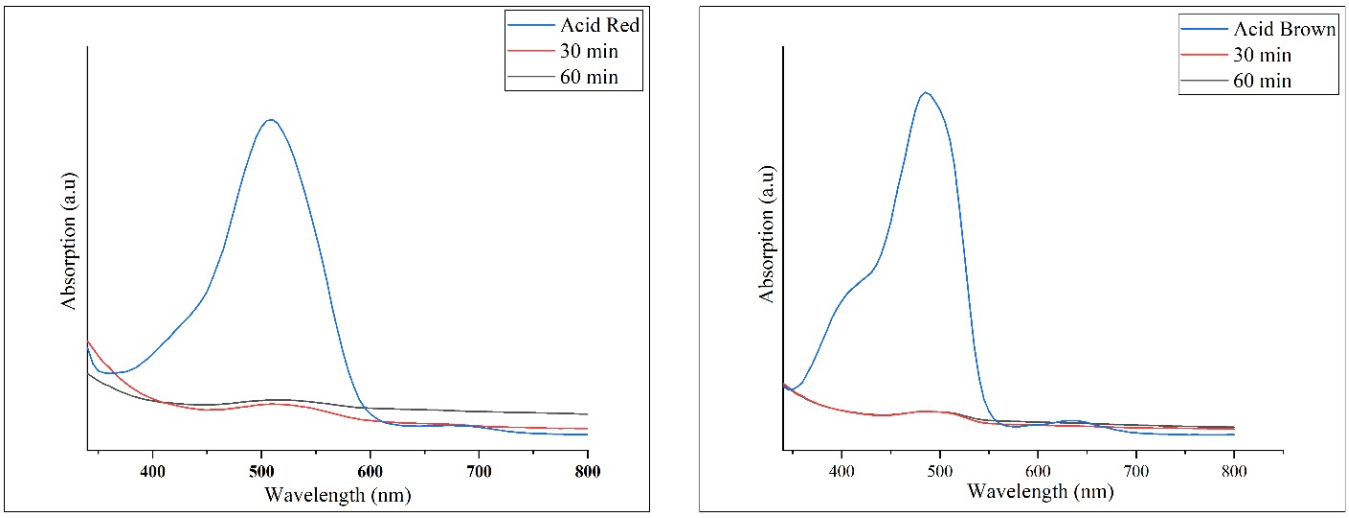

Fig. 6. Photocatalytic activity of the product in degradation of Acid Red (left) and Acid Brown (right)

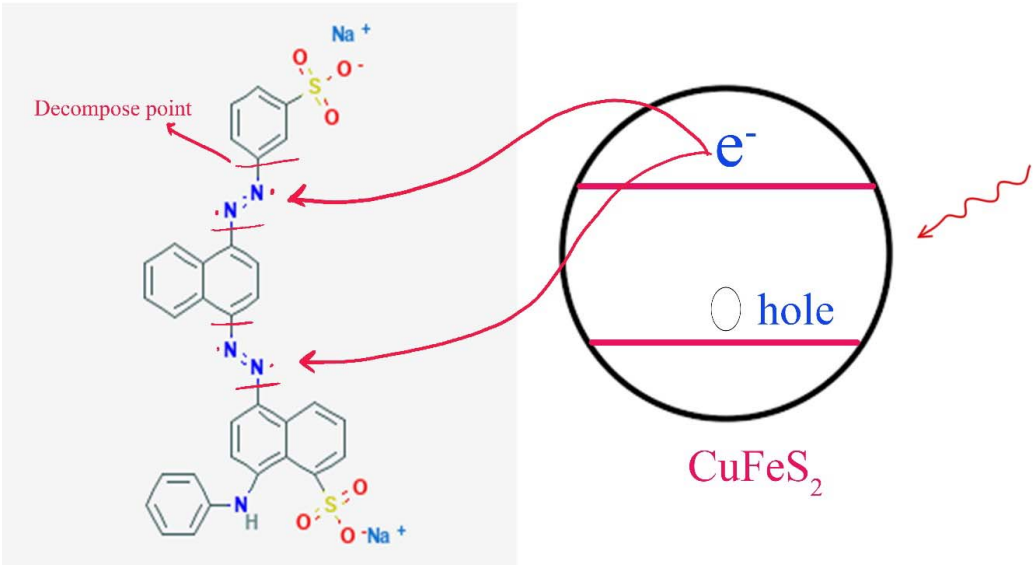

Scheme 2. The mechanism of dye degradation in presence of $CuFeS_2$ photocatalyst

product. It was found the product is composed from crystallites with tetragonal phase and 45.5 nm size. Also, it was found the synthesized product has pure and there are no impurities in its structure. The product size and morphology were studied by TEM analysis and the results showed the product was composed of 20-40 nm and high uniform particles. Finally, the photocatalytic activity of the synthesized $CuFeS_2$ was studied by degradation of Acid brown and Acid red as dyes and it was observed the product has high photocatalytic activity and it can degradate the mentioned dyes with 100 percent.

REFERENCES

[1] E. Dutková, Z. Bujňáková, J. Kováč, I. Škorvánek, M.J. Sayagués, A. Zorkovská, J. Kováč Jr, P. Baláž, Adv. Powder Technol. **29**, 1820-1826 (2018).

[2] S. Thinius, T. Bredow, The Journal of Physical Chemistry C. **123**, 3216-3225 (2019).

[3] S. Ghosh, T. Avellini, A. Petrelli, I. Kriegel, R. Gaspari, G. Almeida, G. Bertoni, A. Cavalli, F. Scotognella, T. Pellegrino, Chemistry of Materials **28**, 4848-4858 (2016).

[4] K.M. Deen, E. Asselin, ChemSusChem **11**, 1533-1548 (2018).

[5] H. Takaki, K. Kobayashi, M. Shimono, N. Kobayashi, K. Hirose, N. Tsujii, T. Mori, Materials Today Physics **3**, 85-92 (2017).

[6] Y. Wu, B. Zhou, C. Yang, S. Liao, W.-H. Zhang, C. Li, Chem. Commun. **52**, 11488-11491 (2016).

[7] Y. Li, Y. Wang, B. Pattengale, J. Yin, L. An, F. Cheng, Y. Li, J. Huang, P. Xi, Nanoscale **9**, 9230-9237 (2017).

[8] B. Bhattacharyya, A. Pandey, J. Am. Chem. Soc. **138**, 10207-10213 (2016).

[9] X. Wu, Y. Zhao, C. Yang, G. He, J. Mater. Sci. – Mater. Electron. **50**, 4250-4257 (2015).

[10] K. Deen, E. Asselin, Electrochim. Acta **212**, 979-991 (2016).

[11] S. Sil, A. Dey, S. Halder, J. Datta, P.P. Ray, Performance, J. Mater. Eng. Perform. **27**, 2649-2654 (2018).

[12] W. Ding, X. Wang, H. Peng, L. Hu, Materials Chemistry Physics **137**, 872-876 (2013).

[13] Y.-H.A. Wang, N. Bao, A. Gupta, Solid State Sciences **12**, 387-390 (2010).

[14] J. Hu, Q. Lu, B. Deng, K. Tang, Y. Qian, Y. Li, G. Zhou, X. Liu, Inorg. Chem. Commun. **2**, 569-571 (1999).

[15] E.J. Silvester, T.W. Healy, F. Grieser, B.A. Sexton, Langmuir. **7**, 19-22 (1991).

[16] B. Bhattacharyya, T. Pandit, G.P. Rajasekar, A. Pandey, The Journal of Physical Chemistry Letters. **9**, 4451-4456 (2018).

[17] J. Wojnarowicz, A. Opalinska, T. Chudoba, S. Gierlotka, R. Mukhovskyi, E. Pietrzykowska, K. Sobczak, W. Lojkowski, Journal of Nanomaterials **2016**, (Article ID=2789871) 1-15 (2016).

[18] I.S. Lyubutin, C.-R. Lin, S.S. Starchikov, Y.-J. Siao, M.O. Shaikh, K.O. Funtov, S.-C. Wang, Acta Mater. **61**, 3956-3962 (2013).

[19] M. Wang, L. Wang, G. Yue, X. Wang, P. Yan, D. Peng, Materials Chemistry Physics **115**, 147-150 (2009).

[20] S.D. Disale, S.S. Garje, Appl. Organomet. Chem. **23**, 492-497 (2009).